Lysozyme-Coupled Poly(poly(ethylene glycol) methacrylate)-Stainless Steel Hybrids and Their Antifouling and Antibacterial Surfaces

ARTICLE *in* LANGMUIR · FEBRUARY 2011

Impact Factor: 4.46 · DOI: 10.1021/la104442f · Source: PubMed

7 AUTHORS, INCLUDING:

Shaojun Yuan
Sichuan University
56 PUBLICATIONS **1,058** CITATIONS
SEE PROFILE

Simo O Pehkonen
University of Eastern Finland
103 PUBLICATIONS **3,630** CITATIONS
SEE PROFILE

Yen-Peng Ting
National University of Singapore
132 PUBLICATIONS **4,296** CITATIONS
SEE PROFILE

Langmuir

ARTICLE

pubs.acs.org/Langmuir

Lysozyme-Coupled Poly(poly(ethylene glycol) methacrylate)−Stainless Steel Hybrids and Their Antifouling and Antibacterial Surfaces

Shaojun Yuan,*[,†] Dong Wan,[‡] Bin Liang,[†] S. O. Pehkonen,*[,§] Y. P. Ting,[‡] K. G. Neoh,[‡] and E. T. Kang[‡]

[†]College of Chemical Engineering, Sichuan University, Chengdu 610065, China

[‡]Department of Chemical and Biomolecular Engineering, National University of Singapore, Singapore 119260, Singapore

[§]CEWIC, Thule Institute University of Oulu, P. O. Box 7300, FI 90014, Finland

Supporting Information

ABSTRACT: An environmentally benign approach to impart stainless steel (SS) surfaces with antifouling and antibacterial functionalities was described. Surface-initiated atom transfer radical polymerization (ATRP) of poly(ethylene glycol) monomethacrylate) (PEGMA) from the SS surface-coupled catecholic L-3,4-dihydroxyphenylalanine (DOPA) with terminal alkyl halide initiator was first carried out, followed by the immobilization of lysozyme at the chain ends of poly(ethylene glycol) branches of the grafted PEGMA polymer brushes. The functionalized SS surfaces were shown to be effective in preventing bovine serum albumin (BSA) adsorption and in reducing bacterial adhesion and biofilm formation. The surfaces also exhibited good bactericidal effects against *Escherichia coli* and *Staphylococcus aureus*. The concomitant incorporation of antifouling hydrophilic brushes and antibacterial enzymes or peptides onto metal surfaces via catecholic anchors should be readily adaptable to other metal substrates, and is potentially useful for biomedical and biomaterial applications.

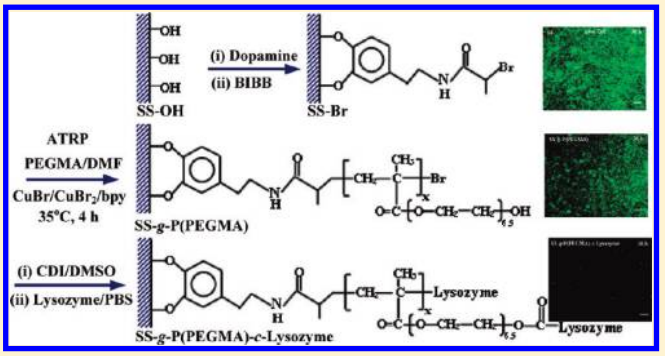

1. INTRODUCTION

Microorganisms tend to adhere strongly to surfaces at the onset of the formation of a complex adhering microbial community, termed a biofilm.[1] Once formed, not only are biofilms extremely resistant to host defense mechanisms or antibiotics, but they also serve as reservoirs for the development of pathogenic infections, leading to devastating complications with high morbidity and treatment costs in biomedical devices and food processing equipment.[2,3] Therefore, increasing attention has been recently paid to altering the surface chemistry via surface modification to prevent bacterial adhesion and decrease the potential for biofilm development.[4−25] Two principal strategies have been developed to generate thin coatings that reduce the initial attachment of bacteria to the solid surfaces: one is to develop antibacterial surface films[4−15] and the other is to immobilize antifouling coatings that resist protein adsorption and subsequently prevent bacterial adhesion onto the surface.[16−28] The techniques employed to generate antibacterial surfaces involve physical entrapment,[4] surface impregnation,[5,6] plasma deposition,[7] polyelectrolytes,[8] or covalent grafting;[9−15] whereas the commonly used approaches for developing nonadhesive coatings are self-assembled monolayers (SAMs)[16−19] or polymer brushes based on poly(ethylene glycol) (PEG) and its derivatives.[20−27] However, even though the antifouling and nonadhesion properties of the PEG-based coatings have been well-documented,[16−25] these coatings have also been reported not to completely prevent bacterial adhesion.[26−28] Accordingly, it is desirable to confer both nonadhesion and antibacterial properties to the substrate surface, upon which nonadhesive functionality can reduce the initial bacterial adhesion, and the antibacterial property can simultaneously eliminate bacterial cells in contact with the surfaces.

Tethering of polymer brushes on a solid substrate is an effective method for modifying the surface properties of the substrate.[29] Among techniques used to prepare polymer brushes, atom transfer radical polymerization (ATRP) is a recently developed "controlled" radical polymerization method. It offers a unique route to dense brushes of narrow polydispersity, controlled architecture, and well-defined thickness and compositions.[29,30] Poly(ethylene glycol) (PEG) brushes are used extensively for the preparation of antifouling surfaces, since they possess many required physical and biochemical properties, such as biocompatibility, nontoxicity, nonantigenicity, and miscibility with many solvents.[31,32] Not only do PEG brushes provide a nonadhesive property, the terminal hydroxyl groups on their side chains can be used for the immobilization of biomolecules.[6]

Received: November 8, 2010
Revised: January 29, 2011
Published: February 21, 2011

Scheme 1. Schematic Diagram Illustrating the Process of Coupling DOPA to SS-OH Surface to Give the SS-DOPA Surface, Immobilization of Alkyl Bromide Initiator via Condensation Reaction (the SS-Br Surface), Surface-Initiated ATRP of PEGMA from the SS-Br Surface (the SS-*g*-P(PEGMA) Surface), Activation of the Hydroxyl Side Chain by 1,1′-Carbonyldiimidazole (CDI) (the SS-*g*-P(PEGMA)-CDI surface) and Subsequent Immobilization of Lysozyme to Produce the SS-*g*-P(PEGMA)-*c*-Lysozyme Surface

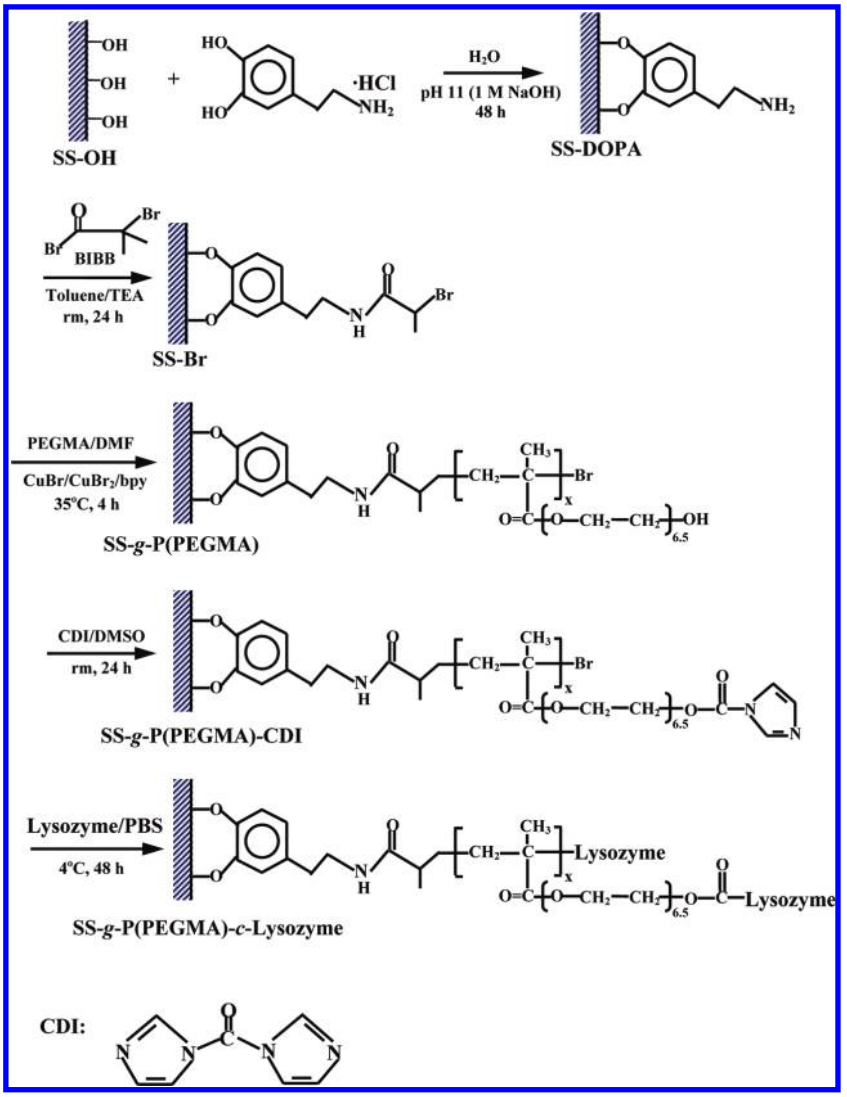

Among the biocides used to inhibit the growth of bacteria, the natural defense substances that are secreted by living organisms, such as hydrolytic enzymes (i.e., protease, glycosidase, and lysozyme), have recently emerged as a particularly attractive class of biocidal agents.[33,34] These enzymes are environmentally benign and act more specifically than conventional biocides, such as antibiotics and quaternary ammonium compounds. Lysozyme, or 1,4-β-*N*-acetylmuramidase, is an enzyme that plays an important role in preventing bacterial infection, especially for Gram-positive bacteria. It can damage bacterial cell walls by catalyzing the hydrolysis of 1,4-β-linkages between *N*-acetylmuramic acid and *N*-acetyl-D-glucosamine residues in a peptidoglycan and between *N*-acetyl-D-glucosamine residues in chitodextrins, increasing the bacteria's permeability and causing the bacteria to burst.[35] Immobilization of lysozyme on polymeric packaging films or stainless steel led to materials displaying antimicrobial properties.[13,35−39] However, few studies have been devoted to concurrent immobilization of an enzyme and PEG chains to confer simultaneously antifouling and antibacterial properties on the solid surfaces.[6,13]

In this study, lysozyme-coupled poly(poly(ethylene glycol) monomethacrylate) (P(PEGMA)) brushes were grafted on stainless steels (SS), via surface-initiated atom transfer radical polymerization (ATRP) of poly(ethylene glycol) monomethacrylate (PEGMA), followed by coupling of an antibacterial lysozyme at the chain end of PEG branches via the 1,1′-carbonyldiimidazole (CDI) as a biofunctional linker, to render their surface antifouling and antibacterial properties. The surface functionalization process is shown in Scheme 1. Although two recent studies have reported the immobilization of peptides or lysozyme on a PEG-based matrix for preparing antibacterial and antifouling coatings,[6,13] there is significant difference between the earlier studies and the current study. The main novelty of this study involved the following: (i) the P(PEGMA) brushes were

anchored onto the SS substrate surface via robust bidentate surface complexes. The catecholic L-3,4-dihydroxyphenylalanine (DOPA), a major component of natural glue proteins secreted by mussels,[40] was used to anchor an alkyl bromine-containing ATRP initiator onto the SS surface, due to its capability to anchor functional biomolecules and polymer brushes onto a large variety of surfaces, such as glasses, metals, and metal oxides.[14,18,19,41,42] (ii) Controlled/living radical polymerization (i.e., "grafting from" approach), instead of using "grafting to" approach previously,[13] was used to synthesize the well-defined P(PEGMA) brushes from SS surfaces. (iii) The antibacterial effectiveness of the lysozyme immobilized on the P(PEGMA) brushes to Gram-negative bacteria was determined, which has never been studied previously. Thus, the antifouling behavior of the resulting surfaces was evaluated from their protein adsorption test, while the antibacterial functionality was assessed from their biocidal activities against Gram-negative *Escherichia coli* (*E. Coli*) and Gram-positive *Staphylococcus aureus* (*S. aureus*) bacteria.

2. EXPERIMENTAL SECTION

2.1. Materials. Type 304 stainless steel plates of 3-mm-thickness were purchased from Metal Samples Co. (Munford, AL). Poly(ethylene glycol) monomethacrylate (PEGMA) macromonomer (M_n ~360), 3, 4-dihydroxyphenylalanine (dopamine), 2,2′-bipyridine (bpy), 2-bromoisobutyryl bromide (BIBB), triethylamine (TEA, 98%), CuBr (99%), $CuBr_2$ (98%), and 1,1′-carbonyldiimidazole (CDI, 97%) were obtained from Sigma-Aldrich Chemical Co. (St. Louis, MO) and were used without further purification. Solvents, such as *N*,*N*′-dimethylformamide (DMF, >99.8%), dimethyl sulfoxide (DMSO, 98%), tetrahydrofuran (THF), ethanol, and acetone were of analytical grade, and were used as received. Water in toluene and TEA was removed by reaction with metallic sodium. Bovine serum albumin (BSA), fluorescein isothiocynate (FITC)-conjugated BSA (BSA-FITC), and lysozyme from chicken egg white (≥40 000 units/mg protein) were obtained from Sigma-Aldrich Chemical Co. (St. Louis, MO). All other chemical reagents and solvents were used as received. Yeast extract, peptone, agar, and beef extract were purchased from Oxoid (Hampshire, UK). *E. Coli* (ATCC, 14948) and *S. aureus* (ATCC, 25923) were obtained from American Type Culture Collection (Manassas, VA, USA). The Live/Dead BacLight bacterial viability kit L131152 was purchased from Molecular Probes, Inc. (Eugene, Oregon, USA). Phosphate buffered saline (PBS) (containing 4.68 g/L of NaH_2PO_4 and 8.662 g/L of Na_2HPO_4, pH of 7.0) was prepared fresh and sterilized in an autoclave before use.

2.2. Surface-Initiated ATRP of PEGMA and Immobilization of Lysozyme. The dopamine was anchored on the hydroxyl-enriched SS (SS-OH) substrates to give rise to the SS-DOPA surface, as well as to provide reactive amine groups for the immobilization of an alkyl bromine ATRP initiator (i.e., SS-Br surfaces). Details for the preparation of SS-OH, SS-DOPA, and SS-Br surfaces are described in Supporting Information. For the grafting of PEGMA polymer (P(PEGMA)) brushes on the SS-Br surface, surface-initiated ATRP of PEGMA was carried out using a [PEGMA (4 mL)]:[CuBr]:[$CuBr_2$]:[bpy] molar feed ratio of 100:1:0.2:2 in 4 mL of DMF solution at 35 °C in a Pyrex tube containing the SS-Br substrates. The reaction was allowed to proceed for 4 h to generate the SS-*g*-P(PEGMA) hybrids. At the end of the reaction, the substrates were washed sequentially with copious amount of DMF and deionized water. The SS-*g*-P(PEGMA) substrates were subsequently immersed in a large volume of ethanol for about 48 h to ensure the complete removal of the physically adsorbed polymer, if any.[43]

For the immobilization of lysozyme on the substrate surfaces, the SS-*g*-P(PEGMA) substrates were immersed in 5 mL of dried DMSO, containing 1 g of CDI, in a Pyrex tube for 24 h at room temperature to give rise to the SS-*g*-P(PEGMA)-CDI surfaces. After their removal from the reaction mixture, the resulting substrates were rinsed with copious amounts of THF and deionized water, and subsequently introduced into 5 mL of the PBS solution containing 2 mg/mL of lysozyme. The immobilization reaction was allowed to proceed at 4 °C for 48 h to produce the SS-*g*-P(PEGMA)-*c*-Lysozyme hybrid surface. After the reaction, the lysozyme-immobilized substrates were washed thoroughly with an excess of the PBS solution and deionized water to remove the physically adsorbed lysozyme, prior to being dried in a vacuum desiccator under reduced pressure overnight.

2.3. Surface Characterization. The composition of the surface-functionalized substrates was determined by X-ray photoelectron spectroscopy (XPS). The XPS measurements were performed on a Kratos AXIS Hsi spectrometer with an Al KR X-ray source (1486.6 eV photons), using procedures similar to those described previously.[21] Static water contact angles of various substrate surfaces were measured at 25 °C and 60% relative humidity using the sessile drop method with a 3 mL water droplet and a telescopic goniometer (model 100-00-(230), Rame-Hart, Inc., Mountain Lake, NJ). The telescope with a magnification power of 23× was equipped with a protractor of 1° graduation. The contact angles reported were the mean values from four substrates, with the value of each substrate obtained by averaging the contact angles from at least three surface locations.

2.4. Protein Adsorption Test. To estimate the antiadhesive or repellent effect of PEG-functionalized substrates (including the SS-*g*-P(PEGMA) and the SS-*g*-P(PEGMA)-*c*-Lysozyme surfaces) toward proteins, the protein adsorption test was performed using BSA and BSA-FITC. This protein was chosen due to its well-known strong adsorption capacity on many types of materials, in particular, stainless steel.[21,26] Typically, the BSA and BSA-FITC were dissolved separately in the PBS solution at a concentration of 2 mg/mL. The pristine SS, SS-*g*-P(PEGMA) and SS-*g*-P(PEGMA)-*c*-Lysozyme substrates were rinsed initially with PBS to rehydrate the surfaces, prior to being placed in one of the protein solutions.[44] The adsorption was allowed to proceed at room temperature for 16 and 48 h, respectively. At the predetermined time, the substrates were removed from the BSA solution, gently washed four times with the PBS solution, and rinsed twice with deionized water to remove the PBS salt. After being dried under reduced pressure, the protein-adsorbed surfaces were characterized by XPS. The XPS N 1s core-level spectrum has been extensively used as a marker for the analysis of the relative amount of adsorbed protein on the stainless steel surface.[21,44] The adsorption of the BSA-FITC on the pristine SS and surface-functionalized substrates was imaged with a Leica DMLM fluorescence microscope (Leica Microsystems, Wetzlar, Germany), equipped with an excitation filter of 495 nm and an emission filter of 525 nm.

2.5. Antibacterial Activity Determination. Two bacterial strains of a Gram-negative *E. Coli* and a Gram-positive *S. aureus* were used to evaluate the capability of the surface-functionalized substrates to kill bacterial cells by contract using the live/dead two-color fluorescence method and in vitro antibacterial test (the survival ratio of viable cells). The two bacterial strains used for the antibacterial assays were cultured in yeast−dextrose broth (containing 10 g/L of peptone, 8 g/L of beef extract, 5 g/L of NaCl, 5 g/L of glucose, and 3 g of yeast extract at a pH of 6.8) at 37 °C.[45] The bacteria-containing broth was centrifuged at 571 × *g* (2700 rpm) for 10 min, and after the removal of the supernatant, the bacterial cells were washed twice with PBS and then resuspended in PBS at a concentration of 10^7 cells/mL. The bacterial cell concentration based on a standard calibration with the assumption that the optical density of 1.0 at 540 nm is equivalent to about 10^9 cells/mL.[46] All the SS substrates and glassware were sterilized with UV irradiation for 1 h prior to the experiment.

For the waterborne antibacterial assays with fluorescence microscopy (FM), the Live/Dead BacLight Bacterial Viability Kits, consisting of a

Table 1. Static Water Contact Angles of the Pristine and Surface-Functionalized SS Substrates

sample	surface composition (molar ratio)	static water contact angle (mean ± SD[i], °)
Pristine SS[a]	−	51 ± 3
SS-OH[b]	−	21 ± 2
SS-DOPA[c]	[C−N]:[C−O]:[C−H][h] = 1.1:2.0:5.0 (1:2:5)	49 ± 3
SS-Br[d]	[C−N]:[C−O/C−Br]:[O═C−NH]:[C−H][h] = 1.03:2.6:0.8:6.0 (1:3:1:6)	54 ± 2
SS-*g*-P(PEGMA)[e]	[C−H]:[O═C−O]:[C−O][h] = 4.3:1.0:11.4 (3:1:12)	33 ± 2
SS-*g*-P(PEGMA)-CDI[f]	[[C−N]:[C−O]:[O═C−O]:[C−H][h] = 1.04:7.7:1.0:5.3	37 ± 3
SS-*g*-P(PEGMA)-*c*-Lysozyme[g]	[C−N]:[C−O]:[O═CNH]:[O═C−O]:[C−H][i] = 1.0:3.7:1.4:0.5:4.9	40 ± 1

[a] Pristine SS corresponds to a newly polished stainless steel (SS) coupon. [b] SS-OH was obtained after the newly polished SS coupon treated in the piranha solution for 30 min. [c] SS-DOPA corresponds to the DOPA-immobilized SS surface after the SS-OH surface reacted with dopamine in mildly basic solutions for 48 h at room temperature. [d] SS-Br was obtained after the SS-DOPA surface reacted with 2-bromopropionyl bromide in toluene solution containing triethylamine for 24 h at room temperature. [e] Reaction conditions: [PEGMA]:[CuBr]:[$CuBr_2$]:[Bpy] = 100:1:0.2:2 in DMF-PEGMA solution (1/1, v/v) at 35 °C for 4 h. [f] SS-*g*-P(PEGMA)-CDI was obtained after the SS-*g*-P(PEGMA) reacted with 1,1′-carbonyldiimidazole (1 g) in 5 mL of DMSO for 24 h at room temperature. [g] SS-*g*-P(PEGMA)-*c*-Lysozyme was obtained after the SS-*g*-P(PEGMA) hybrid coupled with Lysozyme in 2 mg/mL PBS solution of Lysozyme for 48 h at 4 °C. [h] Determined from the XPS curve-fitted C 1s core-level spectra. Values in parentheses are the theoretical ratios. [i] SD denotes standard deviation.

mixture of SYTO 9 green fluorescent nucleic acid dye and propidium iodide (PI) red fluorescent nucleic acid dye, were used. The SYTO 9 is cell membrane permeable and therefore stains both the viable and nonviable bacteria, whereas PI, which has a higher affinity for nucleic acids, is rejected from viable bacterial cells by membrane pumps.[12] When both dyes are present, PI competes with SYTO 9 for nucleic acid binding sites. Thus, viable (appearing green) and dead (appearing red) bacterial cells can be distinguished under the fluorescence microscope. Each SS substrate was immersed in a sterile Erlenmeyer flask containing 5 mL of the bacterial suspension in PBS at a concentration of 10^7 cells/mL. The flask was then shaken at 3.1 × *g* (200 rpm) at 37 °C for 3 and 36 h, respectively. The pristine SS substrates were also immersed in the bacterial suspension as control. After the prescribed incubation time, the substrates were gently washed twice with PBS, and subsequently stained by dropping 0.1 mL solution of the BacLight Kits on the substrate surfaces for 15 min. The stained coupons were imaged under a green filter (excitation/emission, 420−480 nm/520−580 nm) or a red filter (excitation/emission, 480−550 nm/590−800 nm) with a Leica DMLM microscope, equipped with a 100 W Hg lamp. At least three different surface areas were randomly chosen for FM imaging on each substratum to be representative of the entire surface.

To assess the antibacterial properties of the surface-functionalized substrates in a more quantitative manner, an in vitro antibacterial test was carried out as described elsewhere.[45,47] Briefly, the SS substrates were placed in 24-well plates, and 1 mL of bacterial suspension in PBS with an initial cell concentration of 1 × 10^7 cells/mL was pipetted onto the surface of each SS substrate. The bacterial suspension completely covered the substrate surfaces. The well plates were placed in a 25 °C water bath to ensure a wet incubation atmosphere. At predetermined time, the bacterial suspension was collected from the SS substrate surface with pipettes and serially diluted. 0.2 mL aliquots of the serially diluted suspension were plated onto the triplicate solid agar using the spread plate method. After incubation of the plates at 37 °C for 24 h, the number of viable cells (colonies) was counted manually and the results after multiplication with the dilution factor were expressed as the mean colony forming units (CFU) per mL.[47] The survival ratio of bacterial cells was defined as the percentage of viable cells in the bacterial suspension in relative to the total number of the initial cells in the suspension.

3. RESULTS AND DISCUSSION

Stainless steel (SS) surfaces with lysozyme-coupled poly(poly(ethylene glycol) monomethacrylate) (P(PEGMA)) brushes are prepared according to the reaction sequence shown in Scheme 1: (i) dopamine is first coupled to the hydroxyl-enriched stainless steel surface under mildly alkaline conditions to provide the reactive amine groups for the subsequent reaction with 2-bromoisobutyryl bromide to introduce the ATRP initiator, (ii) the P(PEGMA) brushes are covalently grafted from the catecholic initiator-immobilized SS surface via surface-initiated ATRP of poly(ethylene glycol) monomethacrylate (PEGMA), (iii) activation of the hydroxyl of groups of the side chains of P(PEGMA) brushes by 1,1′-carbonyldiimidazole (CDI) to produce the SS-*g*-P(PEGMA)-CDI surface, (iv) covalent immobilization of lysozyme on the SS-*g*-P(PEGMA)-CDI surface to produce the SS-*g*-P(PEGMA)-*c*-Lysozyme surface. Details of each reaction are discussed below.

3.1. Covalent Immobilization of the Catecholic ATRP Initiator on the SS Substrates. As a strong oxidizer, the piranha solution has been widely used to generate an oxidized and hydroxyl-enriched surface on most metals.[43,48] The enrichment of hydroxyl (−OH) groups on the SS surface yields a more hydrophilic substrate surface, as indicated by the decrease in the static water contact angle from 51 ± 3° to 21 ± 2° (Table 1). The X-ray photoelectron spectroscopy (XPS) wide-scan spectrum of the SS-OH surface is composed mainly of O 1s, Cr 2p, and Fe 2p signals from the native surface oxide/hydroxide, as well as a small amount of C 1s arising from adventitious hydrocarbon contamination (Supporting Information, Figure S1). Details on the preparation and characterization of the SS-OH surface had been described earlier.[43]

The use of catechols for surface modification of metallic substrates has been well-documented.[18,19,41,42,49] The mussel adhesive protein dopamine, containing the catechol-end groups, is anchored on the SS substrates via chemisorptions to form a uniform monolayer. The reaction between the OH groups of the hydroxylated oxide and the phenolic OH groups in catechol results in strong bidentate charge-transfer complexes.[50] Parts a−c of Figure 1 show the respective wide scan, C 1s, and N 1s core-level spectra of the dopamine-immobilized SS surface (i.e., the SS-DOPA surface). Successful anchoring of dopamine on the SS substrates can be deduced from the appearance of N 1s and C 1s photoelectron lines in the wide-scan spectrum (Figure 1a), in comparison with that of the SS-OH surface (Supporting Information, Figure S1a). The persistence of signals from the metallic elements indicates that the thickness of the dopamine monolayer

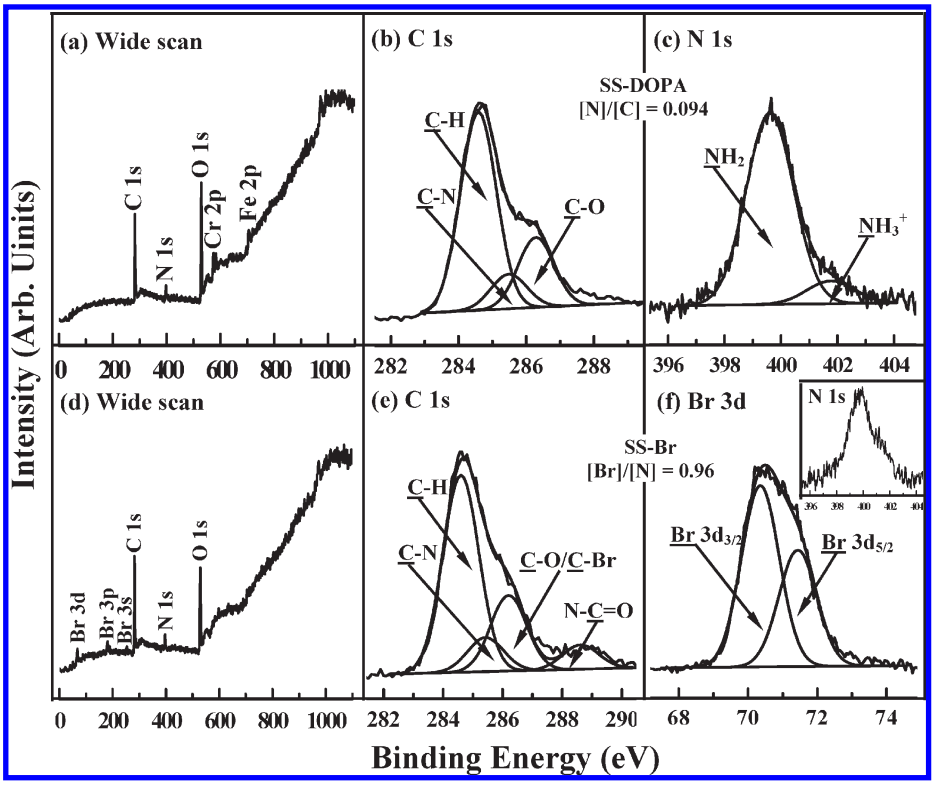

Figure 1. (a) Wide scan, (b) C 1s, and (c) N 1s core-level spectra of the SS-DOPA surface, and (d) wide scan, (e) C 1s, and (f) Br 3d core-level spectra of the SS-Br surface.

is smaller than the probing depth of XPS technique (about 8 nm in an organic matrix[51]). It has been reported previously that the thickness of dopamine monolayer on titanium and stainless steel substrates is about 0.5 nm.[19,49] The C 1s core-level spectrum of the SS-DOPA surface can be curve-fitted into three peak components with binding energies (BEs) at about 284.6, 285.5, and 286.2 eV, attributable to C−H, C−N, and C−O species, respectively (Figure 1b).[51] The area ratio of [C−N]:[C−O]:-[C−H] is around 1.1:2.0:5.0 (Table 1), which is in good agreement with the theoretical value of 1:2:5 for dopamine. The dominant peak component at the BE of 399.6 eV in the curve-fitted N 1s core-level spectrum, attributable to the amine groups, is characteristic of dopamine (Figure 1c).[51] The minor peak component at the BE of 401.7 eV arises from residual $-NH_3^+$ species in the DOPA. The increase in static water contact angle of the substrates from 21 ± 2° to 49 ± 3° is consistent with the coverage of a thin dopamine layer on the SS surface (Table 1). The dopamine-immobilized surface offers the reactive amine groups for the subsequent immobilization of the ATRP initiator.

The introduction of an alkyl bromide ATRP initiator on the SS-DOPA surface is achieved via TEA-catalyzed condensation reaction between surface-anchored amine groups and 2-bromoisobutyryl bromide. Parts d−f of Figure 1 show the wide scan spectrum, C 1s, and Br 3d core-level spectra of the ATRP initiator-immobilized surface (referred to as the SS-Br surface), respectively. The appearance of three additional core-level signals with BEs at about 70, 189, and 256 eV, associated with Br 3d, Br 3p, and Br 3s, respectively,[51] in the wide-scan spectrum indicates successful introduction of the bromide-containing ATRP initiator onto the SS-DOPA surface (Figure 1d). The [Br]:[N] ratio of the surface, as determined from the Br 3d and N 1s core-level spectral area ratio, is about 0.94, indicating that almost all the amine groups have reacted with 2-bromoisobutyryl bromide. This result is further confirmed by the appearance of an amide (O═CNH) species at the BE of 288.4 eV in the curve-fitted C 1s core-level spectrum (Figure 1e). The corresponding Br 3d core-level spectrum of the SS-Br surface with a Br $3d_{5/2}$ BE of 70.4 eV is consistent with the presence of the alkyl bromide species[51] (Figure 1f). The static water contact angle increases slightly from 49 ± 3° for the SS-DOPA surface to 54 ± 2° for the SS-Br surface. Thus, the alkyl bromine groups have been successfully immobilized on the SS-DOPA surface to cater for the subsequent ATRP process from the SS-Br surface.

3.2. Surface-Initiated ATRP of PEGMA and Immobilization of Lysozyme. In this work, the molar ratio of [PEGMA (monomer)]/[CuBr (catalyst)]/[$CuBr_2$ (deactivator)]:[Bpy (ligand)] for the surface-initiated ATRP was controlled at 100:1:0.2:2. The presence of grafted PEGMA polymer (P(PEGMA)) on the SS-Br surface was ascertained by XPS analysis and static water contact angle measurements after the surface had been subjected to vigorous washing and extraction. After 4 h of ATRP, the static water contact angle decreases to 33 ± 2° (Table 1), indicative of an increase in hydrophilicity due to the grafted polymer. Parts a−c of Figure 2 show the wide scan, C 1s, and Br 3d core-level spectra of the P(PEGMA)-grafted SS surfaces (i.e., the SS-*g*-P(PEGMA) surfaces), respectively. The disappearance of N 1s and metallic element signals, together with the significant increase in the intensity of C 1s and O 1s signals, in the wide-scan spectrum (Figure 2a) suggests that the thickness of the P(PEGMA) brushes is greater than the probing depth of XPS technique (about 8 nm in an organic matrix[51]). It has been reported that the thickness of the P(PEGMA) brushes grafted on the silicon surface is around 52 nm after 3 h of ATRP of PEGMA

dx.doi.org/10.1021/la104442f |*Langmuir* 2011, 27, 2761–2774

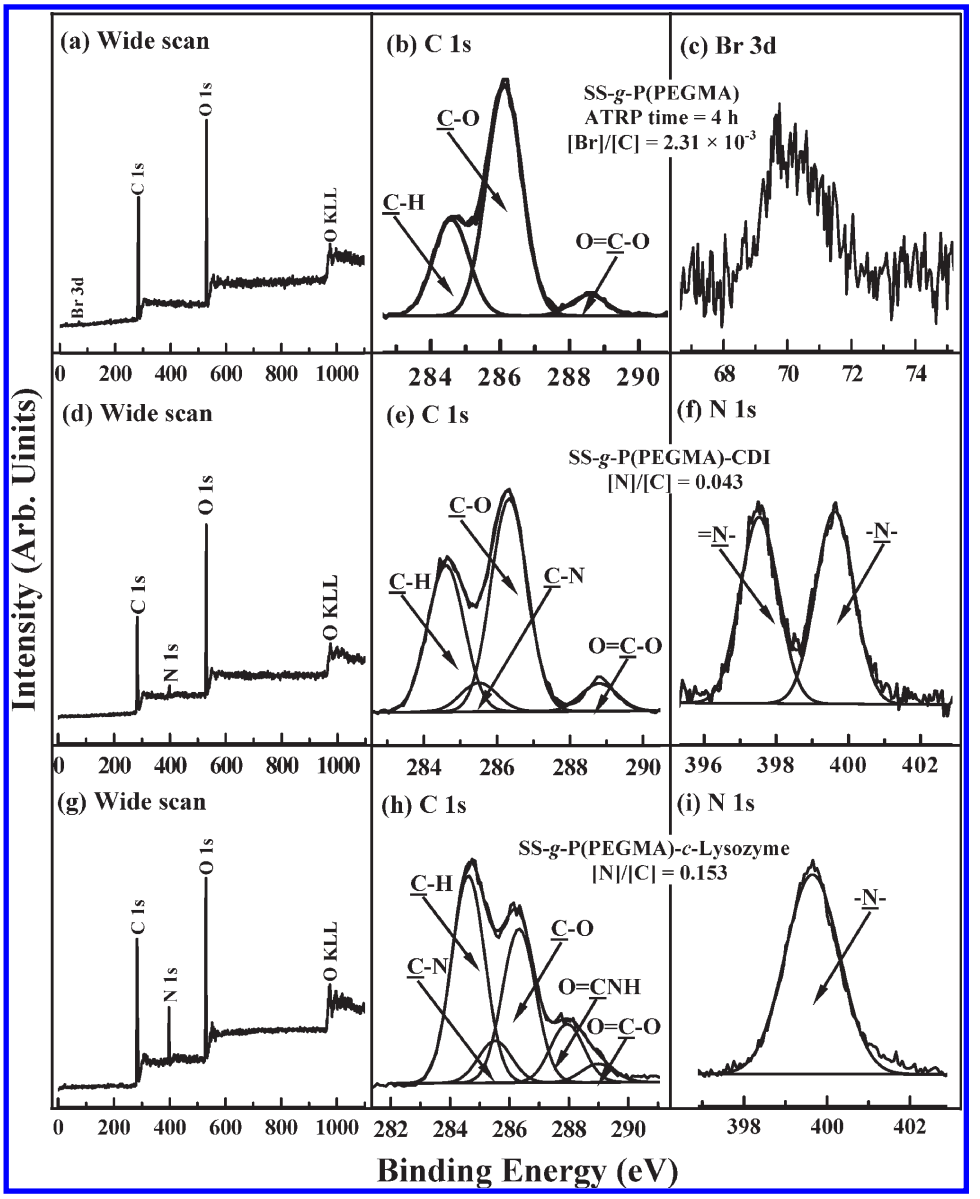

Figure 2. (a) Wide scan, (b) C 1s, and (c) Br 3d core-level spectra of the SS-*g*-P(PEGMA) surface from 8 h of ATRP. (d,g) Wide scan, (e,h) C 1s, and (f,i) N 1s core-level spectra of the SS-*g*-P(PEGMA)-CDI and SS-*g*-P(PEGMA)-*c*-Lysozyme surfaces, respectively.

under similar reaction conditions.[44] The C 1s core-level spectrum of the SS-*g*-P(PEGMA) surface can be curve-fitted into three peak components with BEs at 284.6, 286.2, and 288.9 eV, attributable to C−H, C−O, and O═C−O species, respectively (Figure 2b).[51] The area ratio of the three peak components is about 4.3:11.4:1.0, which is comparable to the expected theoretical value of 3:12:1 for the PEGMA units. The persistence of the Br 3d core-level signal (Figure 2c) is consistent with the fact that the "living" chain end from the ATRP process involves a dormant alkyl halide group, which can be reactivated to initiate the subsequent block copolymerization.[29,30] The quantity of polymers cleaved from the solid surface did not allow an accurate analysis of the molecular weight and molecular weight distribution by gel permeation chromatography.[52]

The reactive hydroxyl groups on the side chains of PEG-based polymer brushes have recently been used to load biomolecules, such as antibacterial peptides and enzymes, to introduce new functionality.[6,13] In this work, the hydroxyl groups of the P(PEGMA) brushes are activated via 1,1′-carbonyldiimidazole (CDI) to generate the SS-*g*-P(PEGMA)-CDI surface. The imidazole carbamate groups on the SS-*g*-P(PEGMA)-CDI surface can react readily with amine-containing biomolecules to form stable carbamate linkages.[44,53] The reactive imidazole carbamate groups hydrolyze very slowly in water at pH 4−8 and can last for more than 6 days in the PBS buffer solution,[53] thus providing a good opportunity for coupling biomolecules in an aqueous buffer solution. Parts d−f of Figure 2 show the respective wide-scan spectrum, C 1s, and N 1s core-level spectra of the SS-*g*-P(PEGMA)-CDI surface. The reappearance of N 1s signal in the wide scan spectrum of the SS-*g*-P(PEGMA)-CDI surface (Figure 2d), in comparison with that of the SS-*g*-P(PEGMA) surface, indicates the successful immobilization of CDI. The C 1s core-level spectrum can be curve-fitted into four peak components with BEs at about 284.6, 285.5, 286.2, and 289.0 eV, attributable to the C−H, C−N, C−O, and O═C−O species, respectively (Figure 2e).[44,51] The N 1s spectrum consists

dx.doi.org/10.1021/la104442f |*Langmuir* 2011, 27, 2761–2774

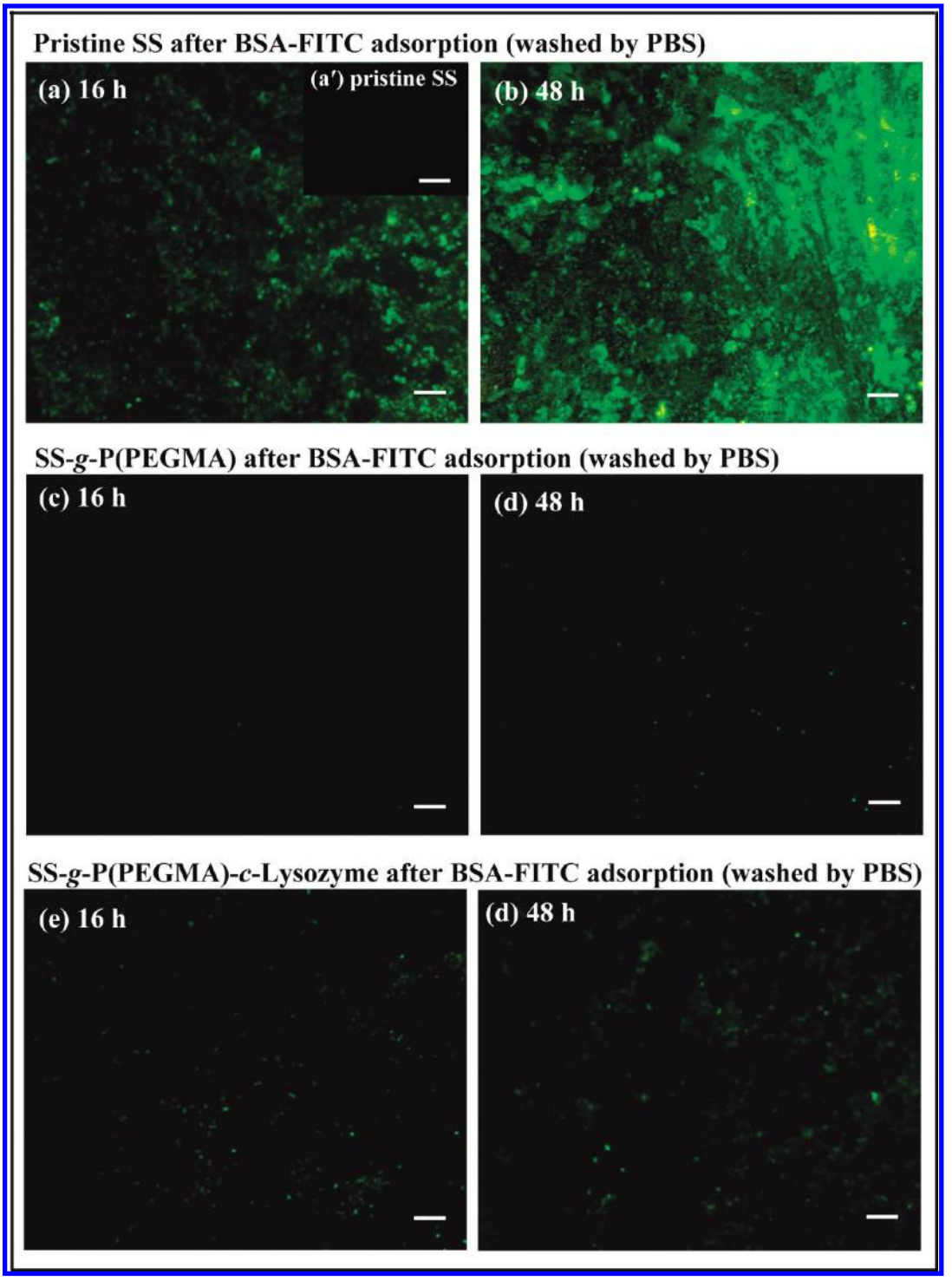

Figure 3. Representative fluorescence microscopy images of the (a,b) pristine SS, (c,d) SS-*g*-P(PEGMA), and (e,f) SS-*g*-P(PEGMA)-*c*-Lysozyme surfaces after being exposed to BSA-FITC solutions for 16 and 48 h, respectively. Scale bars: 100 μm. Inset (a′) shows the fluorescence image of the pristine SS surface before protein adsorption.

of the imine (═N−, at a BE of about 397.5 eV) and amine (−N−, at a BE of about 339.6 eV) components (Figure 2f),[51] associated with CDI. The [N]/[C] ratio, determined from the sensitivity factor-corrected N 1s and C 1s core-level spectral area ratio, is about 0.043. The above results are consistent with the successful activation of the −OH groups of the grafted P(PEGMA) brushes by the imidazole carbamate groups. Furthermore, the [C−N]:[C−O] peak component area ratio of the SS-*g*-P(PEGMA)-CDI surface is about 0.106. Thus, it can be readily concluded that about 36% of hydroxyl groups on the PEGMA repeat units have been activated by CDI on the basis of the chemical structure of PEGMA and CDI.

Covalent coupling of lysozyme on the SS-*g*-P(PEGMA)-CDI surface via the reaction between the amine groups of lysozyme

dx.doi.org/10.1021/la104442f |*Langmuir* 2011, 27, 2761–2774

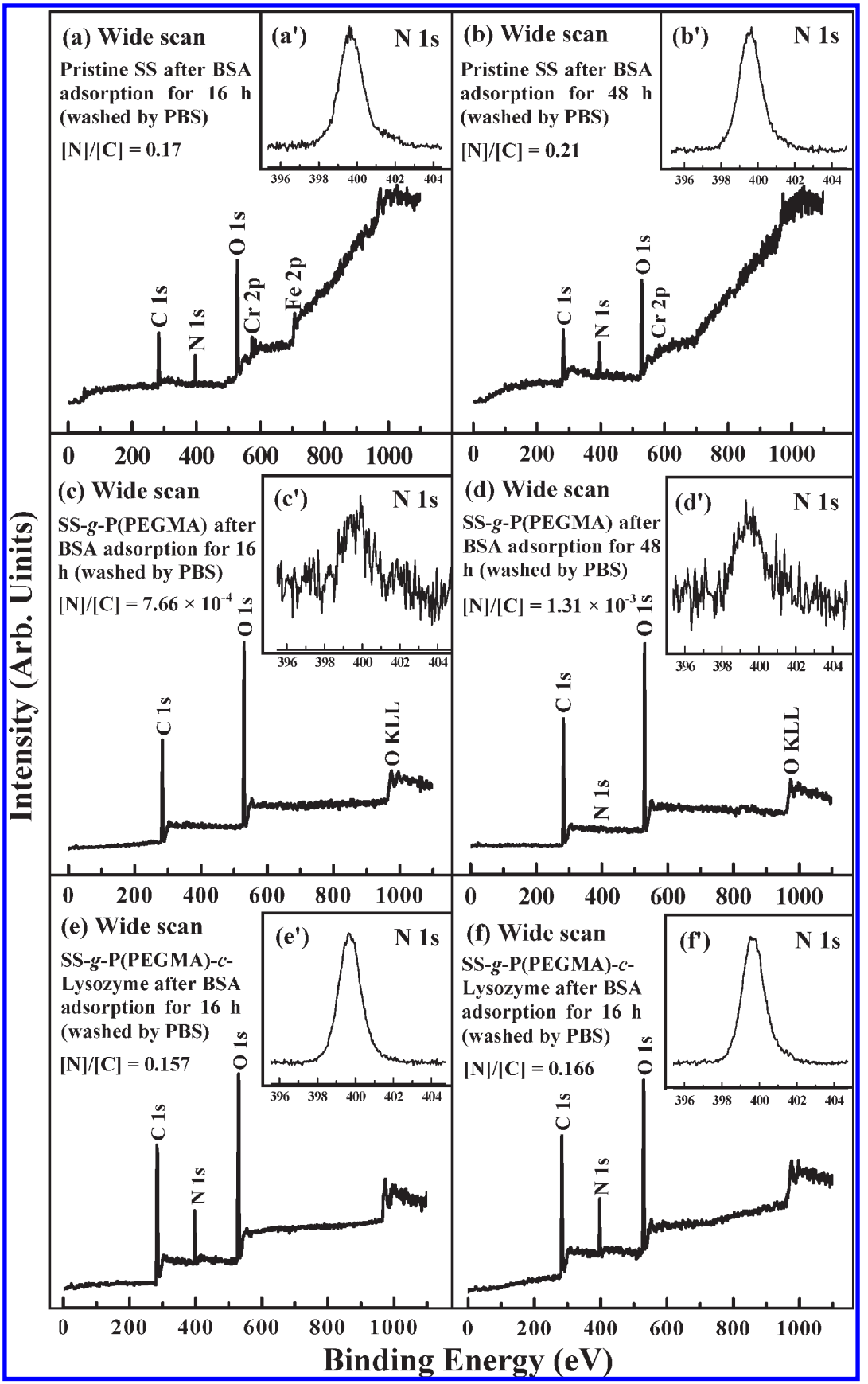

Figure 4. Wide-scan and N 1s core-level spectra of the (a,a′,b,b′) pristine SS, (c,c′,d,d′) SS-*g*-P(PEGMA), and (e,e′,f,f′) SS-*g*-P(PEGMA)-*c*-Lysozyme surfaces (washed by PBS after protein adsorption) after being exposed to BSA solutions for 16 and 48 h, respectively.

dx.doi.org/10.1021/la104442f |*Langmuir* 2011, 27, 2761–2774

and the imidazole carbamate groups produces the SS-*g*-P(PEGMA)-*c*-Lysozyme surface. Parts g−i of Figure 2 show the wide scan, C 1s, and N 1s core-level spectra of the SS-*g*-P(PEGMA)-*c*-Lysozyme surface, respectively. For the SS-*g*-P(PEGMA)-*c*-Lysozyme surface, the C 1s and N 1s spectral line shapes are substantially different from those of the corresponding SS-*g*-P(PEGMA)-CDI. The curve-fitted C 1s core-level spectrum is composed of five peak components with BEs at about 284.6, 285.5, 286.2, 288.2, and 289.1 eV, attributable to the C−H, C−N, C−O, O═CNH, and O═C−O species, respectively (Figure 2h).[44,52] The C−N and O═CNH peak components are associated with lysozyme. The strong N 1s core-level spectrum with a BE at 399.8 eV is attributed to the amine groups of the lysozyme (Figure 2i). The [N]/[C] ratio, determined from the sensitivity factor-corrected N 1s and C 1s core-level spectral area ratio, is about 0.153, comparable to the theoretical value of 0.194 for the chemical structure of lysozyme. The results indicate that a significant amount of lysozyme has been covalently immobilized on the substrate surface. The percentage of monomer unit grafted by lysozyme was quantitatively estimated by the XPS results to be about 25% for the P(PEGMA) brushes. The water contact angle of the SS-*g*-P(PEGMA)-*c*-Lysozyme surface is 40 ± 1°. Thus, the SS-*g*-P(PEGMA)-*c*-Lysozyme surface with the dense P(PEGMA) polymer brushes and the incorporated lysozyme is achieved. The surface is subsequently used for evaluating the antifouling and biocidal efficiency of the surface-functionalized SS substrates.

3.3. Protein Adsorption. To assess the protein adsorption behavior of different substrate surfaces, the pristine SS, the SS-*g*-P(PEGMA), and the SS-*g*-P(PEGMA)-*c*-Lysozyme substrates were exposed to 2 mg/mL PBS solutions of BSA-FITC for 16 and 48 h, and subsequently imaged with a fluorescence microscope. Figure 3 shows the corresponding fluorescence images of the (a,b) pristine SS, (c,d) SS-*g*-P(PEGMA), and (e,f) the SS-*g*-P(PEGMA)-*c*-Lysozyme surfaces. Prior to protein adsorption, no fluorescence was observed from the pristine SS surface (Figure 3a′). However, after 16 h of the protein adsorption, uniform and intense fluorescence is observed across the pristine SS surface (Figure 3a), indicative of a significant extent of BSA-FITC adsorption on the substrate surface. Upon prolonging the exposure time to 48 h, the fluorescence intensity is substantially increased (Figure 3b), associated with the increased extent of the BSA-FITC adsorption on the pristine SS surface. For the SS-*g*-P(PEGMA) surface, almost no fluorescence is observed from the entire surface after 16 h of protein adsorption (Figure 3c), and only faint fluorescence is visible after 48 h of BSA-FITC adsorption (Figure 3d), indicating that the P(PEGMA)-functionalized surface exhibits high efficiency in resisting protein adsorption. Sparsely distributed and scattered fluorescence is observed from the SS-*g*-P(PEGMA)-*c*-Lysozyme surface after 16 and 48 h of BSA-FITC adsorption (Figure 3e and f, respectively), suggesting that there are only finite amounts of protein adsorbed on the substrate surface. The result indicates that the coupled lysozyme has only a limited effect on the antifouling ("biologically inert") efficacy of the grafted P(PEGMA) brushes. Thus, the expected protein-resistant property has been highly retained on the SS-*g*-P(PEGMA)-*c*-Lysozyme surface.

To evaluate the extent of protein adsorption on different substrates in a more quantitative manner, the chemical composition of the protein-adsorbed surfaces was analyzed by XPS. The N 1s core-level signal can be used as a marker for the analysis of the relative amount of adsorbed protein on the substrate surface.[21,44] The wide-scan (a,b) and N 1s (a′, b′) core-level spectra of the pristine SS surface after 16 and 48 h of BSA adsorption are shown in Figure 4. These surfaces were washed with PBS to remove the weakly adsorbed proteins. In comparison with the wide-scan spectrum of the pristine SS surface prior to protein adsorption (Supporting Information, Figure S2a), the appearance of a strong N 1s signal at BE of about 399.8 eV after 16 and 48 h of protein adsorption indicates that a significant amount of protein has been adsorbed on the pristine SS surface (Figure 4a′,b′). The [N]/[C] ratio, as determined from the sensitivity factor-corrected N 1s and C 1s core-level spectral area ratio, is commonly used to represent the relative amount of protein adsorbed on the surface. The [N]/[C] ratio increases from 0 (Supporting Information, Figure S2b and S2c) prior to exposure to BSA to about 0.17 and 0.21, respectively, after 16 and 48 h of protein adsorption (Figure 4a′,b′), indicating that the pristine SS has a strong affinity for proteins, and the amounts of the adsorbed protein increase with increasing exposure time. This result is further ascertained by the change in the C 1s spectral line shape before and after protein adsorption (Supporting Information, Figures S2b, S3a, and S3b). The amine (C−N) and amide (O═CNH) components in the curve-fitted C 1s core-level spectrum after the protein adsorption is characteristic of the adsorbed protein on the pristine SS surface (Supporting Information, Figures S3a and S3b). The strong affinity of the pristine stainless steel for protein is well-known.[21] Most surfaces will bind proteins, but the type and amount of protein binding depends on the physicochemical nature of the surface. The metal surface binds soluble proteins first through fixed charge interactions, and the strength of specific binding remains fairly high. As a result, the process of protein adsorption on stainless steel surfaces is irreversible.[54]

After 16 and 48 h of exposure to the BSA solution and washed by PBS, the N 1s signals are barely discernible in the wide-scan spectra of the SS-*g*-P(PEGMA) surface (Figure 4c,d). The corresponding [N]/[C] ratios are about 7.7×10^{-4} and 1.3×10^{-3}, respectively. These negligible nitrogen signals indicate that the surface-grafted P(PEGMA) brushes possess antifouling properties against protein adsorption. The almost unchanged C 1s line shape before and after BSA exposure further confirms the resistance of the grafted P(PEGMA) brushes to the protein adsorption (Supporting Information, Figures S2c and S2d). The effectiveness of the SS-*g*-P(PEGMA) surface in reducing protein adsorption is associated with the unique properties of the PEG units,[21,44,49] such as minimum free energy at the polymer/water interface, almost unlimited solubility, high mobility, large excluded volume, and hydrophilicity, which can substantially reduce the ionic interaction and hydrogen bonding of the PEG units with protein molecules. Moreover, the large excluded volume of the PEG units and the highly mobile or flexible PEG chains in water also tend to repel protein molecules approaching the substrate surface.[55] Thus, the grafted P(PEGMA) brushes render the stainless steel surface with the unique ability to reduce protein adsorption. Parts e,e′,f,f′ of Figure 4 show the wide scan (e,f) and N 1s core-level (e′,f′) spectra of the SS-*g*-P(PEGMA)-*c*-Lysozyme surface after 16 and 48 h of protein adsorption. No significant change can be observed in the wide-scan spectra before and after the protein adsorption (Figures 2g and 4e,f). The respective [N]/[C] ratios (as determined from the sensitivity factor-corrected N 1s and C 1s core-level spectral area ratio) are about 0.157 and 0.166, respectively, after 16 and 48 h of adsorption in the BSA solution. Both ratios are comparable to

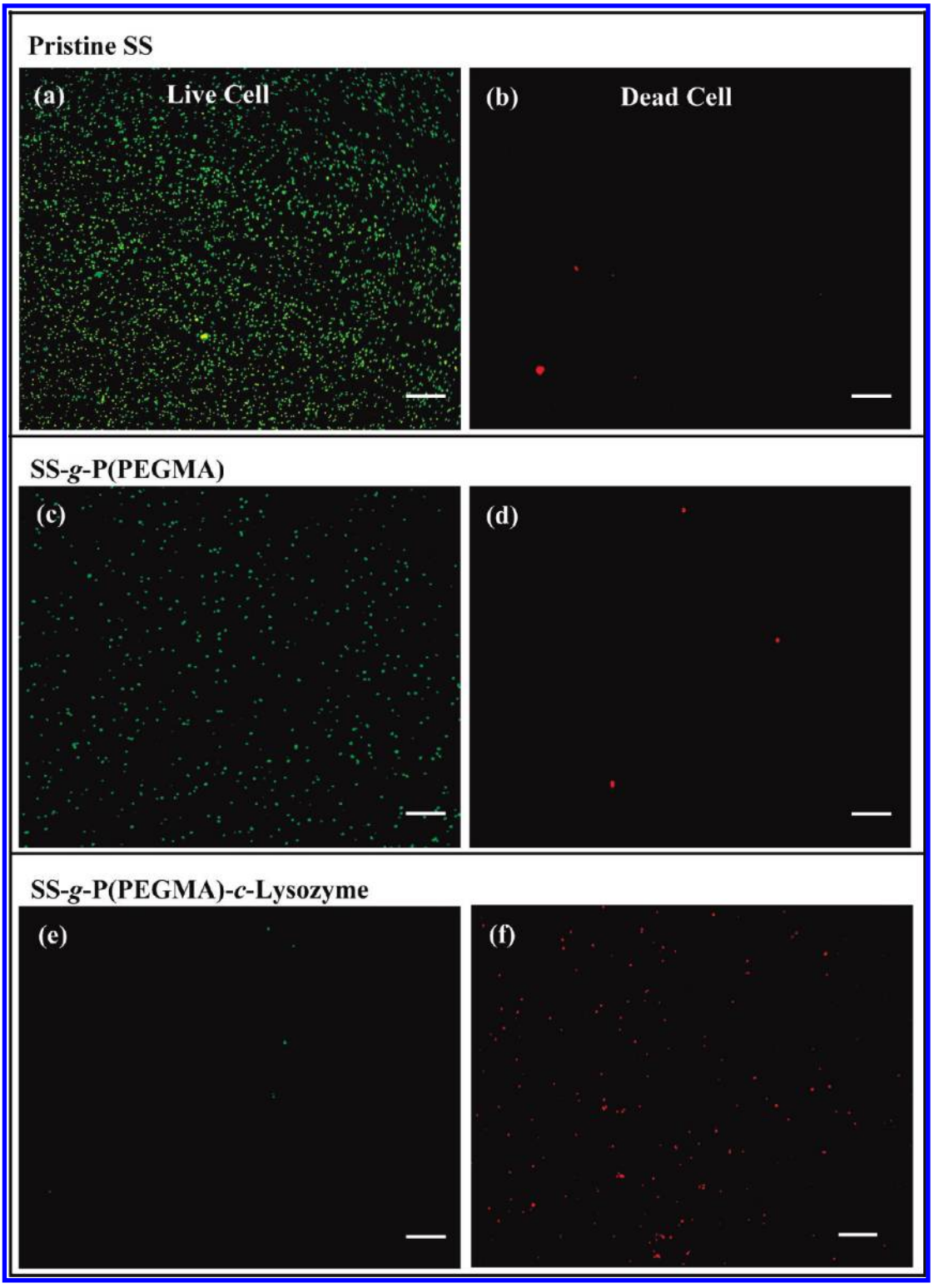

Figure 5. Representative fluorescence microscopy images of *S. aureus* for the pristine SS, SS-*g*-P(PEGMA), and SS-*g*-P(PEGMA)-*c*-Lysozyme surfaces under the green filter (a,c,e) and the red filter (b,d,f), respectively, after 3 h of exposure.

that of the SS-*g*-P(PEGMA)-*c*-Lysozyme surface (0.153) prior to protein adsorption. No significant change in C 1s line shapes can be observed before and after protein adsorption, albeit of a small increase in the intensity of the amide components after 48 h of protein adsorption (Supporting Information, Figures S3f). The above results indicate that, after the BSA exposure, the N signals on the SS-*g*-P(PEGMA)-*c*-Lysozyme surface originate mainly from the covalently coupled lysozyme rather than the adsorbed BSA protein. The slight increase in [N]/[C] ratios (~0.012 after 48 h of protein adsorption) indicates that only a finite amount of proteins have been adsorbed on the SS-*g*-P(PEGMA)-*c*-Lysozyme surface. The protein-resistant nature

dx.doi.org/10.1021/la104442f |*Langmuir* 2011, 27, 2761–2774

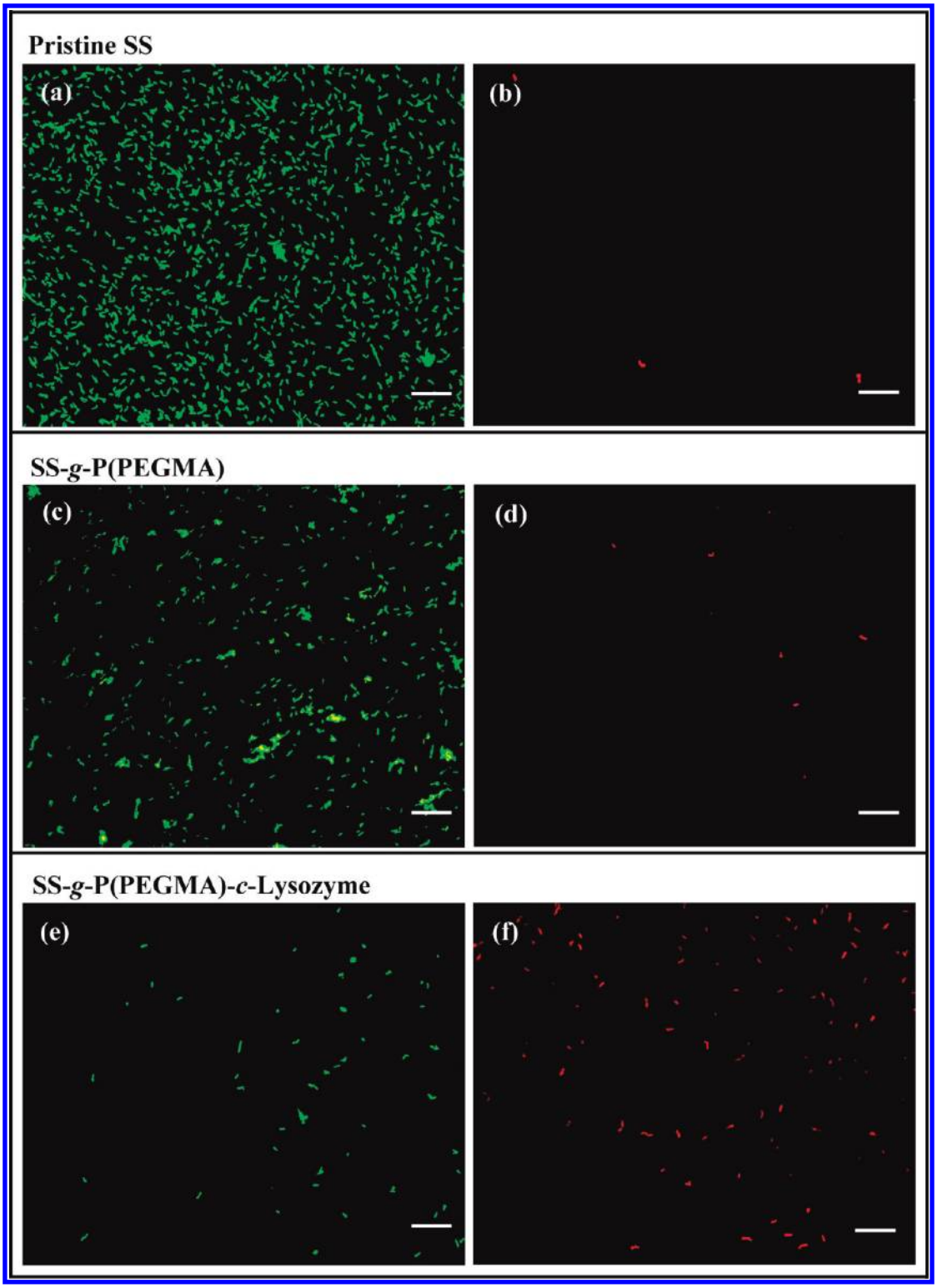

Figure 6. Representative fluorescence microscopy images of *E. Coli* for the pristine SS, SS-*g*-P(PEGMA), and SS-*g*-P(PEGMA)-*c*-Lysozyme surfaces under the green filter (a,c,e) and the red filter (b,d,f), respectively, after 3 h of exposure.

of the SS-*g*-P(PEGMA)-*c*-Lysozyme surface has thus also been observed. The above XPS results are also consistent with the fluorescence spectroscopy results of Figure 3.

3.4. Determination of Antibacterial Characteristics of Functionalized Surfaces. The ability of the functionalized surfaces to kill bacteria was tested for both *E. Coli* and *S. aureus* using the live/dead two-color fluorescence method and in vitro antibacterial assays. For the waterborne antibacterial assays with fluorescence microscopy (FM) images, the distribution of viable and dead bacteria on the pristine and surface-functionalized SS substrates, after immersion in a *S. aureus* and *E. Coli* suspension of 10^7 cells/mL for 3 and 36 h at 37 °C, was observed by staining

dx.doi.org/10.1021/la104442f |*Langmuir* 2011, 27, 2761–2774

with a combination dye of SYTO 9 and PI, as shown in Figure 5 and Figure 6, respectively. The images reveal that there is a clear distinction between the number of *S. aureus* or *E. Coli* cells on the pristine and functionalized substrates. Numerous readily distinguishable bacterial cells with green fluorescence, either individually or in small clusters, are distributed on the pristine SS surface after 3 h of immersion in the *S. aureus* or *E. Coli* suspension (Figures 5a and 6a), while only several single cells with red fluorescence can be observed for both bacterial stains (Figures 5b and 6b), indicating that most of the bacterial cells are viable with the cell membrane intact on the pristine SS surface. Upon prolonging the exposure time to 36 h, the bacterial clusters with green fluorescence (viable cells) grow dense and aggregate to form thick biofilms on the pristine SS surface for both bacterial strains (Supporting Information, Figures S3a and S4a). At the same time, a good many of bacterial cells with red fluorescence (dead cells) are discernible on the pristine SS surface (Supporting Information, Figures S3b and S4b). These dead cells are mainly associated with natural apoptosis during the bacterial growth process. The above results reveal that the stainless steel surfaces are a good substrate for the adhesion and proliferation of microorganisms, and biofilm formation will occur readily on such materials in contact with bacteria.

For the SS-*g*-P(PEGMA) surfaces, the density of viable cells (stained green) for each bacterial strain appears to be lower than that of the pristine SS surface after 3 h of immersion in a suspension (Figures 5c and 6c), indicating that bacterial adhesion is markedly reduced by the grafted P(PEGMA) brushes during the initial immersion period. The presence of only a few single cells with red fluorescence indicates the absence of biocidal functionality of the P(PEGMA) brushes (Figures 5d and 6d). It has been reported that the reduction of bacterial adhesion by the PEG-grated surfaces is related to their low surface energy and high surface hydrophilicity.[20,23] However, upon prolonging the exposure time to 36 h, substantially more viable cells of *S. aureus* or *E. Coli* (stained green) are distributed over the SS-*g*-P(PEGMA) surfaces to form patchy biofilms (Supporting Information, Figures S3c and S4c), while the presence of dead cells (stained red) on the substrate surface is due to natural apoptosis rather than antibacterial activity during the bacterial growth process (Supporting Information, Figures S3d and S4d). This result is consistent with the previous findings that, in spite of possessing the antiadhesive characteristics for reducing bacterial adhesion, the PEG-based surfaces cannot completely prevent bacteria adhesion and biofilm formation.[26−28] However, the PEGMA polymer brushes tethered on the SS substrates are less effective in reducing bacterial adhesion than those grafted from the silicon or glass substrates in previous studies.[56,57] This phenomenon is probably associated with the relatively lower grafting density of the P(PEGMA) brushes, essentially caused by the low initiator density on the SS surface. It should be noted that there is no significant difference in the extent of adhesion between Gram-negative *E. Coli* and Gram-positive *S. aureus* bacteria on the pristine SS and SS-*g*-P(PEGMA) surfaces. Although the mechanism of microbial adhesion to material surfaces has not been fully elucidated, interactions of bacteria with material surfaces can arise from electrostatic and Lifshitz−van der Waals forces, hydrophobic interactions, and a variety of specific receptor-adhesion interactive forces.[15,23,25−28,56]

As for the SS-*g*-P(PEGMA)-*c*-Lysozyme substrates, after 3 h of exposure in a *S. aureus* or *E. Coli* suspension, only a few viable cells (stained green) are sparsely distributed on the substrate surfaces (Figures 5e and 6e), and the majority of bacteria cells are dead cells with red fluorescence (Figures 5f and 6f), indicative of the presence of antibacterial property on the substrate surface. The bacterial density (including viable and dead cells) of the SS-*g*-P(PEGMA)-*c*-Lysozyme surface is also found to be significantly lower than that of the corresponding pristine SS surface, indicative of the inhibition of bacterial adhesion on the SS-*g*-P(PEGMA)-*c*-Lysozyme surface. It has been reported previously that the presence of biomolecules, such as peptides[6,15,58] and enzymes,[13] bound onto PEG do not influence the adhesion of bacteria. Another important findings for the SS-*g*-P(PEGMA)-*c*-Lysozyme surface is that this surface differs substantially in antibacterial activity against *S. aureus* and *E. Coli*. Almost all the viable cells of *S. aureus* are killed by the surface-bearing lysozyme, as shown in Figure 5e. Even prolonging the exposure time to 36 h, only a few sparsely distributed single viable cells of *S. aureus* (stained green) are observed on the SS-*g*-P(PEGMA)-*c*-Lysozyme surface (Supporting Information, Figure S3e), indicative of the high efficiency of the surface-coupled lysozyme in killing Gram-positive *S. aureus*. For the Gram-negative *E. Coli*, after 3 h of exposure to the bacterial culture, sparsely distributed individual viable cells (stained green) are observed on the substrate surface, indicating that a few of *E. Coli* cells can survive on the SS-*g*-P(PEGMA)-*c*-Lysozyme surface (Figure 6e). With the increase in exposure time to 36 h, substantially more viable cells of *E. Coli* are visible on the substrate surface (Supporting Information, Figure S4e), although a high concentration of bacterial cells and small-sized bacterial colonies with red fluorescence (dead cells) are also spotted on the substrate surfaces (Supporting Information, Figure S4f.). The killing efficiency of the surface-bearing lysozyme to *E. Coli* is thus lower than that to *S. aureus*. The results are consistent with the previous finding that lysozyme, as an enzyme with antibacterial properties, possesses strong antibacterial activity against Gram-positive bacteria rather than Gram-negative bacteria, due to the difference in the structure of their cell walls.[35,37] The current study further confirms that the lysozyme immobilized on the side chains of P(PEGMA) brushes is also lethal to Gram-negative *E. Coli* bacteria on contact. Thus, the antibacterial property of the SS-*g*-P(PEGMA)-*c*-Lysozyme surface is ascertained .

To further ascertain the killing efficiency of the SS-*g*-P(PEGMA)-*c*-Lysozyme surface in a more quantitative manner, an in vitro antibacterial test was also carried out as described earlier. Parts a and b of Figure 7 show the effect of contact time on the survival ratio of *S. aureus* and *E. Coli* on the pristine SS, SS-*g*-P(PEGMA), and SS-*g*-P(PEGMA)-*c*-Lysozyme surfaces. The number of viable cells in the *S. aureus* or *E. Coli* suspension decreases by less than 10% for both bacterial strains after 4 h in contact with the pristine SS and SS-*g*-P(PEGMA) surfaces. This relatively minor reduction may have resulted from natural apoptosis. On the other hand, in the presence of SS-*g*-P(PEGMA)-*c*-Lysozyme surface, the viable cell number of *S. aureus* has decreased by more than 60% after 2 h. After 4 h of exposure, more than 95% of the cells are no longer viable (Figure 7a). On the other hand, the numbers of *E. Coli* viable cells decrease by about 40% after 2 h, and about 80% of *E. Coli* cells have been killed after 4 h in contact with the lysozyme-immobilized surface (Figure 7b). These results further demonstrate that the lysozyme-immobilized surface exhibits a high bactericidal efficiency against the Gram-positive *S. aureus* and slightly reduced efficiency against *E. Coli* on contact. The in vitro

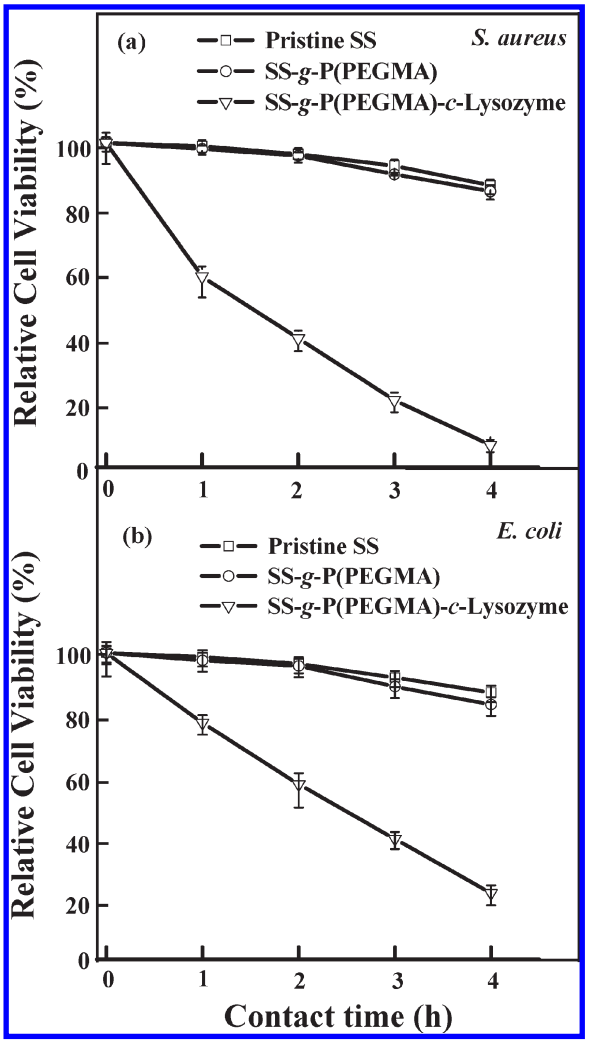

Figure 7. Survival rates of viable (a) *S. aureus* and (b) *E. Coli* cells in PBS at 37 °C as a function of time in contact with the different substrates. The cell number was determined by the surface-spread method. The error bars represent the standard deviation calculated from three independent experiments.

antibacterial test results are thus consistent with those from fluorescence microscopy.

3.5. Stability of Functionalized Substrate Surface and Persistence of Activity. In order to check the persistence of antibacterial activity of the coatings, it is appropriate to emphasize on the stability of the grafted lysozyme-coupled P(PEGMA) layers on the SS substrate surface. In this work, a self-assembled monolayer of DOPA was chemisorbed onto the SS surface to anchor the grafted P(PEGMA) brushes. The robustness of the DOPA monolayer, attributable to the strong affinity of bidentate charge-transfer complexes,[50] has been well-documented.[14,15,18,19] Moreover, the well-defined polymer brushes grafted on various substrate surfaces, including glass, fiber, paper, silicon wafer, SS, and titanium, via surface-initiated ATRP have been shown to be stable under harsh environments.[19,24,29,30] Consequently, the high stability of the SS-*g*-P(PEGMA)-*c*-Lysozyme surface is predictable.

To further investigate the possible release of the lysozyme immobilized on the side chains of the P(PEGMA) brushes, the SS-*g*-P(PEGMA)-*c*-Lysozyme sample was immersed in 15 mL of the PBS solution at 25 °C for 10 days under slight agitation. After the predetermined time, the SS sample was washed vigorously with deionized water and dried under reduced pressure prior to XPS characterization. The XPS results reveal that the composition of the SS-*g*-P(PEGMA)-*c*-Lysozyme surface remained practically unchanged after immersion in the PBS solution (Supporting Information, Figure S5). The [N]/[C] ratio of about 0.151 is virtually equal to the precedent value of 0.153 for the SS-*g*-P(PEGMA)-*c*-Lysozyme surface before PBS immersion (Figure 2i), indicative of no lysozyme leaching out of the biocidal coatings. Thus, the high stability of the lysozyme on the P(PEGMA) brushes is ascertained.

Furthermore, the above SS-*g*-P(PEGMA)-*c*-Lysozyme sample was also assayed for antibacterial activity, using the same bacteria and the same protocol as those described in the Experimental Section. The results show that the lysozyme-coupled P(PEGMA) layers retain a high killing efficiency toward both Gram-positive *S. aureus* and Gram-negative *E. Coli* bacteria, thus confirming the persistence of antibacterial activity of the lysozyme functionalized surface. In addition, further studies focusing on the long-term antibacterial performance of the lysozyme-coupled P(PEGMA) layers in the growth medium are in progress to evaluate the prevention of biofilm formation in relevant media.

4. CONCLUSIONS

Environmentally friendly antifouling and antibacterial coatings were prepared from antifouling P(PEGMA) brushes, immobilized by biomimetic anchors inspired by the mussel adhesive protein (dopamine) and side chain end-functionalized with a natural defensive enzyme, hen egg white lysozyme. The catecholic dopamine was first immobilized on the stainless steel surface for anchoring an alkyl bromine ATRP initiator. The P(PEGMA) brushes were subsequently grafted from the bromine-terminated stainless steel surface via surface-initiated ATRP of PEGMA. The hydroxyl groups on the side chains of P(PEGMA) brushes were then activated with CDI to covalently immobilize the antibacterial lysozyme. The so-functionalized SS-*g*-P(PEGMA)-*c*-Lysozyme hybrid surface displayed high antifouling activity toward the BSA protein as compared to the pristine stainless steel surface. The lysozyme-functionalized surface also exhibited a high bactericidal efficiency toward both Gram-positive *S. aureus* and Gram-negative *E. Coli* bacteria in contact with the surface, as revealed by antibacterial assays. Thus, the desired antifouling property of both the P(PEGMA) brushes and the bactericidal effect of lysozyme were preserved to resist protein adsorption and to prevent bacterial adhesion, proliferation, and biofilm formation. The environmentally friendly and nonreleasing approach to achieve these two important functions simultaneously will be highly advantageous in combating biofilm-related infections, and will be potentially useful for biomedical and biomaterial applications.

■ ASSOCIATED CONTENT

Supporting Information. Additional information as described in the text. This material is available free of charge via the Internet at http://pubs.acs.org.

■ AUTHOR INFORMATION

Corresponding Author

*To whom all correspondence should be addressed. Tel: +86-28-85460557, Fax: +86-28-85460557, E-mail: yuanshaojun@gmail.com (S. J. Yuan); simo.pehkonen@oulu.fi (S.O. Pehkonen).

■ ACKNOWLEDGMENT

The authors would like to thank Sichuan University for the financial support of this study under the Research Starting Fund 208-220-413-4022.

■ REFERENCES

(1) Gottenbos, B.; Van der Mei, H. C.; Busscher, H. J. *Methods Enzymol.* **1999**, *310*, 523.
(2) Costerton, W. J.; Cheng, K. J.; Geesey, G. G.; Ladd, T. I.; Nickel, J.; Curtis, D. M.; Marrie, T. J. *Annu. Rev. Microbiol.* **1987**, *41*, 435.
(3) Costerton, W. J.; Stewart, P. S.; Greenberg, E. P. *Science* **1999**, *284*, 1318.
(4) Guyomard, A.; Dé, E.; Jouenne, T.; Malandain, J. J.; Muller, G.; Glinel, K. *Adv. Funct. Mater.* **2008**, *18*, 758.
(5) Etienne, O.; Picart, C.; Taddei, C.; Haikel, Y.; Dimarcq, J. L.; Schaaf, P.; Voegel, J. C.; Ogier, J. A.; Egles, C. *Antimicrob. Agents Chemother.* **2004**, *48*, 3662.
(6) Glinel, K.; Jonas, A. M.; Jouenne, T.; Leprince, J.; Galas, L.; Huck, W. T. S. *Bioconjugate Chem.* **2009**, *20*, 71.
(7) Jampala, S. N.; Sarmadi, M.; Somers, E. B.; Wong, A. C. L.; Denes, F. S. *Langmuir* **2008**, *24*, 8583.
(8) Boulmedais, F.; Frisch, B.; Etienne, O.; Lavalle, P. H.; Picart, C.; Ogier, J. A.; Voegel, J. C. *Biomaterials* **2004**, *25*, 2003.
(9) Ignatova, M.; Voccia, S.; Gabriel, S.; Gilbert, B.; Cossement, D.; Jérôme, R.; Jérôme, C. *Langmuir* **2009**, *25*, 891.
(10) Humblot, V.; Yala, J. F.; Thebault, P.; Boukerma, K.; Héquet, A.; Berjeaud, J. M.; Pradier, C. M. *Biomaterials* **2009**, *30*, 3503.
(11) Lee, S. B.; Koepsel, R. R.; Morley, S. W.; Matyjaszewski, K.; Sun, Y. J.; Russell, A. J. *Biomacromolecules* **2004**, *5*, 877.
(12) Madkour, A. E.; DabkowsKi, J. M.; Nösslein, K.; Tew, G. N. *Langmuir* **2009**, *25*, 1060.
(13) Caro, A.; Humblot, V.; Méthivier, C.; Minier, M.; Salmain, M.; Pradier, C. M. *J. Phys. Chem. B* **2009**, *113*, 2102.
(14) Charlot, A.; Sciannaméa, V.; Lenoir, S.; Faure, E.; Jérôme, R.; Jérôme, C.; Van De Weerdt, C.; Martial, J.; Archambeau, C.; Willet, N.; Duwez, A. S.; Fustin, C. A.; Detrembleur, C. *J. Mater. Chem.* **2009**, *19*, 4117.
(15) Khoo, X. J.; Hamilton, P.; O'Toole, G. A.; Snyder, B. D.; Kenan, D. J.; Grinstaff, M. W. *J. Am. Chem. Soc.* **2009**, *131*, 10992.
(16) Ostuni, E.; Chapman, R. G.; Liang, M. N.; Meluleni, G.; Pier, G.; Ingber, D. E.; Whitesides, G. M. *Langmuir* **2001**, *17*, 5336.
(17) Böcking, T.; Kilian, K. A.; Gaus, K.; Gooding, J. J. *Langmuir* **2006**, *22*, 3494.
(18) Statz, A. R.; Barron, A. E.; Messersmith, P. B. *Soft Matter* **2008**, *4*, 131–139.
(19) Fan, X. W.; Lin, L. J.; Dalsin, J. L.; Messersmith, P. B. *J. Am. Chem. Soc.* **2005**, *127*, 15843.
(20) Dong, B. Y.; Jiang, H. Q.; Manolache, S.; Wong, A. C. L.; Denes, F. S. *Langmuir* **2007**, *23*, 7306.
(21) Zhang, F.; Kang, E. T.; Neoh, K. G.; Wang, P.; Tan, K. L. *Biomaterials* **2001**, *22*, 1541.
(22) Kilian, K. A.; Böcking, T.; Gaus, K.; Gal, M.; Gooding, J. J. *Biomaterials* **2007**, *28*, 3055.
(23) Park, K. D.; Kim, Y. S.; Han, D. K.; Kim, Y. H.; Lee, E. H. B.; Suh, H.; Choi, K. S. *Biomaterials* **1998**, *19*, 851.
(24) Hu, F. X.; Neoh, K. G.; Cen, L.; Kang, E. T. *Biomacromolecules* **2006**, *7*, 809.
(25) Müller, R.; Eidt, A.; Hiller, K. A.; Katzur, V.; Subat, M.; Schweikl, H.; Imazato, S.; Ruhl, S.; Schmalz, G. *Biomaterials* **2009**, *30*, 4921.
(26) Jiang, W.; Ravn, D. B.; Gram, L.; Kingshott, P. *Colloids Surf., B* **2003**, *32*, 275.
(27) Roosjen, A.; Boks, N. P.; van der Mei, H. C.; Busscher, H. J.; Norde, W. *Colloids Surf., B* **2005**, *46*, 1.
(28) Kingshott, P.; Jiang, W.; Bagge-Ravn, D.; Gadegaard, N.; Gram, L. *Langmuir* **2003**, *19*, 6912.
(29) Edmondson, S.; Osborne, V. L.; Huck, W. T. S. *Chem. Soc. Rev.* **2004**, *33*, 14.
(30) Matayjaszewski, K.; Xia, J. H. *Chem. Rev.* **2001**, *101*, 2921.
(31) Singh, N.; Cui, X. F.; Boland, T.; Husson, S. M. *Biomaterials* **2007**, *28*, 763.
(32) Branch, D. W.; Wheeler, B. C.; Brewer, G. J.; Leckband, D. E. *Biomaterials* **2001**, *22*, 1035.
(33) Ibrahim, H. R.; Kato, A.; Kobayashi, K. *J. Agric. Food Chem.* **1991**, *39*, 2077.
(34) Zasloff, M. *Nature* **2002**, *415*, 389.
(35) Appendini, P.; Hotchkiss, J. H. *Package Technol. Sci.* **1997**, *10*, 271–279.
(36) Conte, A.; Buonocore, G. G.; Bevilacqua, A.; Sinigaglia, M.; Del Nobile, M. A. *J. Food Protect.* **2006**, *69*, 866.
(37) Wang, Q.; Fan, X. R.; Hu, Y. J.; Yuan, J. G.; Cui, L.; Wang, P. *Bioproc. Biosyst. Eng.* **2009**, *32*, 633.
(38) Alves, C. R.; Pimenta, M. G. R.; Vieira, R. H. S. F.; Furtado, R. F.; Guedes, M. I. F.; Silva, R. C. B.; Assis, O. B. G. P. *Electron. J. Biotechnol.* **2007**, *10*, 160.
(39) Conte, A.; Buonocore, G. G.; Sinigaglia, M.; Lopez, L. C.; Favia, P.; d'Agostino, R.; Del Nobile, M. A. *J. Food Protect.* **2008**, *71*, 119.
(40) Waite, J. H.; Tranzer, M. L. *Science* **1981**, *212*, 1038.
(41) Lee, H.; Dellatore, S. M.; Miller, W. M.; Messersmith, P. B. *Science* **2007**, *318*, 426.
(42) Lee, H.; Scherer, N. F.; Messersmith, P. B. S. *Proc. Natl. Acad. Sci. U.S.A.* **2006**, *103*, 12999.
(43) Yuan, S. J.; Xu, F. J.; Pehkonen, S. O.; Ting, Y. P.; Neoh, K. G.; Kang, E. T. *J. Electrochem. Soc.* **2008**, *155*, 196.
(44) Xu, F. J.; Liu, L. Y.; Yang, W. T.; Kang, E. T.; Neoh, K. G. *Biomacromolecules* **2009**, *10*, 1665.
(45) Shi, Z. L.; Neoh, K. G.; Kang, E. T. *Biomaterial* **2005**, *26*, 501.
(46) Hogt, A. H.; Dankert, J.; Feijen, J. *J. Biomed. Mater. Res.* **1986**, *20*, 533.
(47) Fu, J. H.; Ji, J.; Yuan, W. Y.; Shen, J. C. *Biomaterials* **2005**, *26*, 6684.
(48) Martin, H. J.; Schulz, K. H.; Bumgardner, J. D.; Walters, K. B. *Langmuir* **2007**, *23*, 6645.
(49) Fan, X. W.; Lin, L. J.; Messersmith, P. B. *Biomacromolecules* **2006**, *7*, 2443.
(50) Martin, S. T.; Kesselman, J. M.; Park, D. S.; Lewis, N. S.; Hoffmann, M. R. *Environ. Sci. Technol.* **1996**, *30*, 2535.
(51) Moulder, J. F.; Strickle, W. F.; Sobol, F. E.; Bomben, K. D. *Handbook of X-ray photoelectron spectroscopy*; Perkin-Elmer Corp.: Eden Prairie, MN, 1992.
(52) Biesalski, M.; Rühe, J. *Macromolecules* **2004**, *37*, 2196.
(53) Crowley, S. C.; Chan, K. C.; Walters, R. R. *J. Chromatogr.* **1986**, *359*, 359.
(54) Van Enmckevort, H. J.; Dass, D. V.; Langdon, A. G. *J. Colloid Interface Sci.* **1984**, *98*, 138.
(55) Kjellander, R.; Florin, E. *J. Chem. Soc., Faraday Trans. 1* **1981**, *77*, 2053.
(56) Roosjen, A.; van der Mei, H. C.; Busscher, H. J.; Norde, W. *Langmuir* **2004**, *20*, 10949.
(57) Kingshott, P.; Wei, J.; Bagge-Ravn, D.; Gadegaard, N.; Gram, L. *Langmuir* **2003**, *19*, 6912.
(58) Wagner, V. E.; Koverstein, J. T.; Bryers, J. D. *Biomaterials* **2004**, *25*, 2247.